Engineering Physics
2021; 5(2): 29-39
http://www.sciencepublishinggroup.com/j/ep
doi: 10.11648/j.ep.20210502.12
ISSN: 2640-1010 (Print); ISSN: 2640-1029 (Online)

Principles of Wheelset Hunting and Construction of Total Solution to Hunting

Jack Youqin Huang

High Tech Pressure Safety, Glen Carbon, Illinois, USA

Email address:
youqinh@hotmail.com, info@htpressuresafety.com

To cite this article:
Jack Youqin Huang. Principles of Wheelset Hunting and Construction of Total Solution to Hunting. *Engineering Physics*. Vol. 5, No. 2, 2021, pp. 29-39. doi: 10.11648/j.ep.20210502.12

Received: July 20, 2021; **Accepted**: August 2, 2021; **Published**: August 12, 2021

Abstract: Wheelset hunting is a motion with two degrees of freedom. The second degree of freedom of hunting is investigated in this paper. Rolling radius difference is commonly understood as the root cause of wheelset hunting. Normally, hunting will begin as soon as the truck begins to move. Rolling radius difference will initiate the hunting and can only be used to determine the configuration of the first quarter of a hunting cycle. Then a mechanism will come into exist to determine the configuration of the second quarter of the hunting cycle, which is exactly the same as the one of first quarter but in the opposite direction. The second half of the hunting cycle is a mirror of the first half. The information from wheelset hunting is too large and too complicated for people to understand and analyze. However, the radius of curvature of wheelset circular motion can be calculated exactly, especially at some special configurations, even though the radius of curvature of wheelset circular motion keeps changing in both magnitude and direction. Furthermore, comparison of the radii of curvature between hunting curve and a cosine curve shows that the curve for the wheelset in hunting motion is sinusoidal. This is proven mathematically in the paper. The limits in Klingel's results were discussed. Due to the fact that Klingel's results are unable to provide a strong theoretical base for further understanding the complicated dynamic characteristics caused by hunting, misleading in hunting is overwhelmed. After understanding the principles of wheelset hunting, three critical speeds in hunting and dynamic loading for truck design in three directions were calculated; wheelset hunting curve while curving was generated; wheelset dynamic interaction was analyzed and the question "Why trains stay on tracks" was answered correctly, just to name a few. Thus, a total solution to the hunting problems can be expected and was discussed in the paper.

Keywords: Wheelset Hunting Curve, Sinusoidal, Truck Hunting, Two Degrees of Freedom, Radius of Curvature, Rolling Radius Difference, Comparison, Total Solution to Hunting

1. Introduction

Truck hunting is referred as to the lateral oscillation of a truck. The subject has been researched for a long time in the railroad industry. Klingel (1883) realized that the conicity caused the hinting and created a formula to calculate the wave length of the lateral oscillation [2],

$$L_k=2\pi(r_o*l/\lambda)^{1/2} \quad (1)$$

In deriving Equation 1, the equation ($d^2y/d^2x=1/R$) is used to begin with. This equation is used to calculate the radius of curvature for a small bending curve is the general practice in engineering, for example, the bending problem of a beam. However, the equation ($d^2y/d^2x=-1/R$) was used to derive Klingel's formula [2]. That is, a minus sign has to be added to the equation for a sinusoidal solution. The next step is to find the relationship between y and R. This was derived from the Retenbacher's formula [2], $y=(r_o l)/(\lambda R)$, as shown in the copy below, Figure 1 (from reference 2).

The problem in Redtenbacher's formula is that the lateral deflection y is ignored in the derivation. If y is ignored, it means that center of wheelset and center of rail are coincident. Then there will be no hunting occurred. So the lateral deflection y must be included in the derivation. Redtenbacher's formula should begin with $(r_o-\lambda y)/(R-l-y)=(r_o+\lambda y)/(R+l-y)$, then one will obtain $y=(r_o l)/(\lambda R)+y^2/R$.

Another way to find the relationship between y and R is to use the calculation of R (see Eq. 3). To use the relationship between R and the major and minor radii, we have $(R-l-y)=2l*r_1/(r_2-r_1)$, with $r_1=r_o-\lambda y$ and $r_2=r_o+\lambda y$. After some mathematical operations, we have $y=(r_o l)/(\lambda R)+y^2/R$.

It is clear that Redtenbacher's formula [$y=(r_o l)/(\lambda R)$] was extracted from the correct formula ($y=(r_o l)/(\lambda R) + y^2/R$) by ignoring a term ($y^2/R$) in it. Thus, a sinusoidal solution can be obtained for the Klingel's formula. If y is very small and R is very large, can the elimination of the term, y^2/R, be justified? Elimination of y^2/R is equivalent to ignoring lateral deflection y in the beginning of the derivation. As just stated, there will be no hunting if y is ignored. Nevertheless, Klingel's formula can only viewed as an engineering approximation not the exact solution. Furthermore, Klingel's formula cannot explain why the hunting motion going from side to side, and Klingel's formula can only have one wheelset configuration to start the hunting motion. It can be seen from this research that there are many wheelset configurations that can initiate the hunting motion.

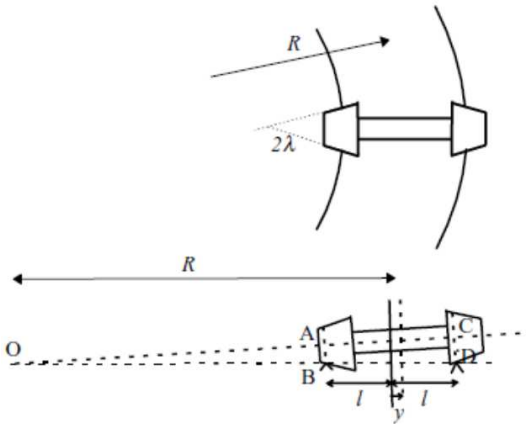

$$OAB = OCD$$

$$(r_0 - \lambda y)/(R - l) = (r_0 + \lambda y)/(R + l)$$

$$y = r_0 l / R\lambda$$

Figure 1. *Wheelset position on track.*

This further research on wheelset hunting is an expanding of a previous research [1] to deal with the 2nd degree of freedom (DOF) of hunting. The previous research analyzed the 1st degree of freedom, while wheelset hunting due to rolling radius difference (RRD) was simulated as a centrifugal pendulum with a fixed radius for the centrifugal motion (Figure 2). The frequency of hunting oscillation for the 1st degree of freedom was given as:

$$\Omega_n = 2V\,[2r_1(r_1-r_2)]^{(0.5)}/[G(r_1+r_2)] \qquad (2)$$

An exact hunting curve for the second degree of freedom will be created in this research, which is totally different than the Klingel's derivation in many ways. Wheelset hunting was further proven to be as a centrifugal pendulum which would switch to the other side of the rail [1]. The repeating of side-switching as the train going forward forms the motion of hunting. There are two reasons that side-switching happens to the centrifugal pendulum: 1). The radius of the centrifugal motion increases from R to ∞, and 2). A mechanism at the neutral state ($r_2=r_1=r$) causes the switching and determines how far the reversal can go. Thus, first quarter part of hunting is determined by the rolling radius difference while second quarter of hunting is mandated by this mechanism. The first half of the hunting curve is then created and the second half of the hunting curve is just a mirror of the first half. The hunting curve for a wheelset is found to be sinusoidal: $y=C*\cos\omega x$.

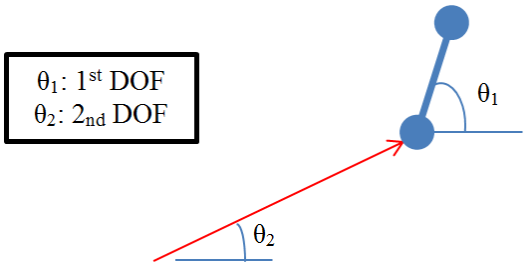

Figure 2. *Wheelset Centrifugal Pendulum.*

Historically, hunting has been connected to creepage. So the creepage problem will be discussed briefly. The creep mechanism is believed to be crucial important in identifying the root cause of hunting by many researchers [2, 3], and is viewed as the guide to hold the wheelset hunting. After understanding the motion states of the wheelset, we can see how and what things go wrong in the originating of the creepage theory [1, 4, 5, 7-11]. In a book [6] (Chapter 2) by Bosso et al., it is illustrated that wheelset motion on the rail is not "pure rolling" and that there is a small sliding occurring at the contact. "The forces arising from this (sliding) motion are therefore indicated as creep forces." However, the sliding on the contact is caused by the oscillation of the 1st DOF of the centrifugal pendulum (as just shown in this paper). The sliding rubbing forces should be and can be calculated by ordinary engineering applications. Furthermore, Bosso presented "The first experiments performed on steam locomotives by Carter in the 1930's", in which it was found that "the sliding condition gradually increased depending on the applied torque". Thus, it is believed that "this was the first observation of creepage". However, what observed is not creepage (or anything it may be called), because the sliding condition will increase with the frequency of the 1st DOF of the oscillation, and the frequency will increase with the velocity or the pulling power.

A key problem for truck hunting is to prove that hunting motion is sinusoidal, because hunting motion is always assumed to be sinusoidal in railroad research and practices. This problem is solved in this further research. That is, the center of the wheelset is in a sinusoidal motion and a mathematical analysis has performed on the motion curve to show that it has the same characteristics as a sinusoidal curve, $y=C*\cos\omega x$. Unlike the Klingel's formula, $y=C*\cos\omega x$ provides a complete set of information to determine exactly the hunting curve. Thus, more and deeper hunting analyses can be done based on this exact hunting curve, such as the hunting interaction between wheelsets in a truck, and the truck hunting dynamic forces and critical speeds in three directions, etc.

2. Wheelset Centrifugal Motion

The idealized model for a wheelset on rail is shown in Figure 3, with weight denoting by W. The wheel treads have a taped angle α, with the center of wheelset not coincident with the center of rail. Thus, the rolling radii would be $r_1$and r_2 respectively. By observation, we can see that the wheelset will do a circular motion.

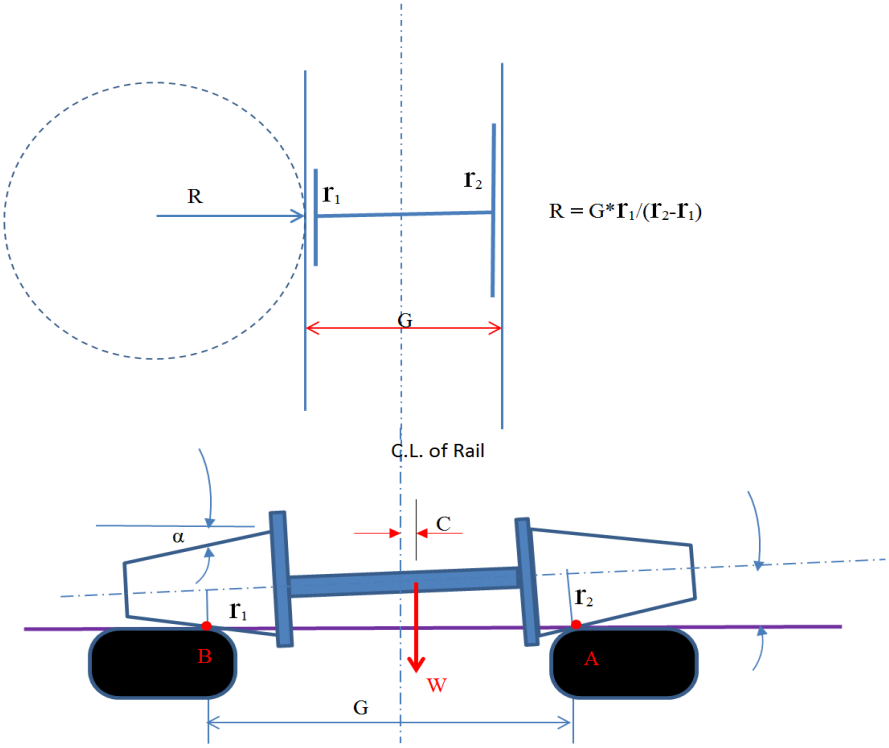

Figure 3. *State of Maximum Potential Energy for the Lateral Motion (α: taper angle of the wheel tread, C. L.: center line).*

Due to there is a difference in the rolling radius (r_1&r_2) between two wheels, theoretically, the wheelset will do a circular motion because r_2 wheel will cover longer distances than r_1 wheel in the same time. This circular motion is the motion of the second degree of freedom and will be studied in the following. The radius of the centrifugal motion can be calculated as

$$R=G*r_1/(r_2-r_1) \quad (3)$$

where G denotes the gauge and r_1 and r_2 represent respectively the rolling radii on two wheels. For the convenience of illustration, r_1 and r_2 are also referred to as minor and major radii respectively.

However, this circular motion is not a simple circular motion. Firstly, the radius of the centrifugal motion, R, will keep changing continuously while the wheelset rolling on the rail. Secondly, the forward direction of wheelset movement will be alternated also. Thirdly, the center of the centrifugal motion of the wheelset will switch side. That is to say, while moving forwards the wheelset will change its moving direction at the same time.

At this stage, it is important to study the change of the wheel/rail contact points A and B. For the purpose of discussion, let's call them the wheel tread contact points also. It can be easily seen that wheel/rail contact points A and B will move forwards on both the wheel and rail. However, it must realize that wheel/rail contact points A and B are always along a straight line on the rail head regardless of the position of the wheelset on the rail. This is due to the fact that the wheel tread rotates and the rail is straight and stable. Distance between wheel tread contact points A and B will keep changed (becomes longer or shorter) because the wheelset will not be perpendicular to the rail due to the centrifugal motion of the wheelset, as will be demonstrated later.

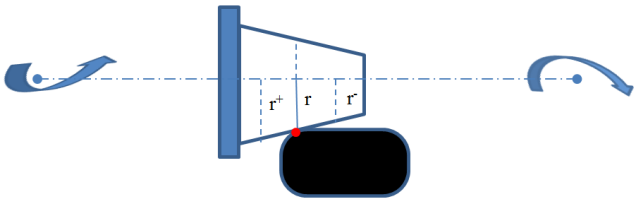

Figure 4. *Change of wheel tread radius in the motion of hunting.*

It is worthwhile to further examine how the wheel tread contact point changes on the surface of the tapered wheel tread. As contact points change, rolling radius of the wheel will change. That is the root cause of the continuous centrifugal motion for the wheelset. At the same time, it is the centrifugal motion that will change the rolling radius of the wheel during its motion, which can be seen from Figure 4. When the centrifugal motion is towards the left of the

wheel, rolling radius r will decrease to r^-. This will happen to the wheel on the right in Figure 3. By the same token, when the centrifugal motion is towards the right, rolling radius r will increase to r^+. This will happen to the wheel on the left in Figure 3. Furthermore, the demonstration shows that the change of the rolling radius depends on the horizontal distance that the wheel tread moves.

3. Analysis of Wheelset Locations in Circular Motions

It is a very tedious task to calculate the exact lateral distance that the wheel tread moves. But that is key to show how and why the rolling radius of the wheel keeps changing. It is found that the wheelset lateral movement is related to the position of the wheelset on the rail after the centrifugal motion.

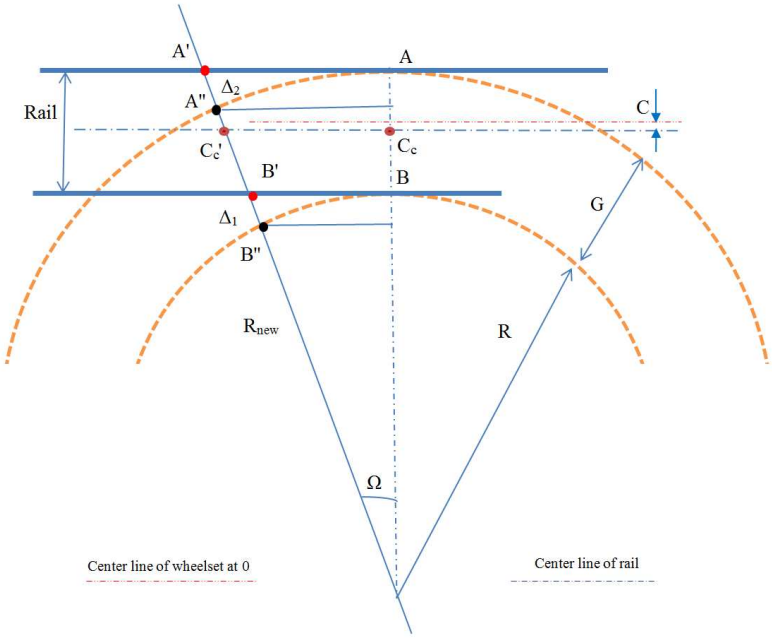

Figure 5. *Wheel Tread/Rail Contact Points in Hunting (Circular Motion Magnified).*

Referring to Figure 5, let's examine the rolling motion for a wheelset with rolling radii r_1 and r_2. The wheelset is the one shown in Figure 3 previously and only the contact points A and B are shown in Figure 5. From the energy point of view, this is the state with maximum potential energy to the circular motion because the center of gravity of the wheelset is at its highest. At the beginning of hunting, the lateral distance between wheel tread contact points A and B is denoted by G. Thus, as demonstrated previously, the wheelset will begin a circular motion. The circular path of the wheelset's motion is depicted in Figure 5. The two straight rails are also represented by the straight lines on which the wheel/rail contact points lie. For the outer wheel, contact points changing from A to point A' corresponds to a circular motion of angle Ω, while for the inner wheel, the wheel/rail contact point will change from B to point B' after angle Ω. In other words, wheel/rail contact points A and B are always along a straight line on the rail. That further proves the previous proclamation about the movement of contact points.

Consequently, lateral distance between contact points A and B, representing by the gauge length G at the beginning of hunting, is replaced by the new distance between contact points A' and B'. For the new wheelset position, the new lateral distance between wheel tread contact points for the wheelset can be calculated as (G/cosΩ). It is becoming longer as stated previously, its center, however, is not on the center line of the gauge unless $r'_1=r'_2=r$ is reached. It should be pointed out that the center of hunting (of the wheelset) is not coincident with the center of the gauge to begin with.

The radius of the centrifugal motion is a function of G. As the lateral distance between wheelset contact points becomes longer, the radius of the centrifugal motion needs to be updated with (G/cosΩ). That is, replacing G with (G/cosΩ) in the calculation of new R, the radius of circular motions. Note that the wheelset motion will still be a centrifugal motion with the new R until a condition of zero RRD is reached.

However, to update R, one needs to realize that both r_1 and r_2 also keep changing in the circular motion. This is because the lateral distance between wheel tread contact points keeps changing in the process of hunting, or in the circular motion.

Therefore, we should compute the lateral displacements for the wheel tread contact points to begin with. It should be noted that, in one way, the wheel/rail contact points are always on the rail and along a straight line, and in the other way, the rail is fixed and the wheelset is in a circular motion. Thus, the lateral movement of wheelset relative to the corresponding rail is exactly the horizontal lateral wheel tread movement, denoting by Δ_1 and Δ_2.

Nevertheless, referring to Figure 5 and assuming R constant, the distances Δ_1 and Δ_2 can be calculated as

$$\Delta_1=R(1/\cos\Omega - 1) \quad (4)$$

$$\Delta_2=(R+G)(1/\cos\Omega - 1) \quad (5)$$

where Δ_1 and Δ_2 represent the distances between points A' and A", and points B' and B" respectively. It can be seen that $\Delta_1 \neq \Delta_2$. That is to say, wheel tread movements in the two wheels are different (slightly) even though they are connected rigidly by an axel, because the wheelset is in a circular motion.

After the circular motion of angle Ω, the rolling radii of the wheelset become (See Figure 6).

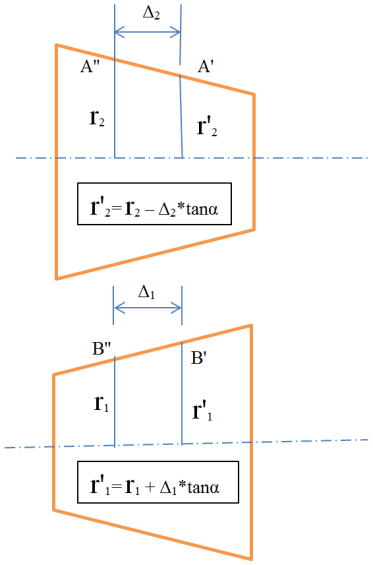

Figure 6. *Calculation for New Rolling Radii.*

$$r'_1=r_1 + \Delta_1*\tan\alpha \quad (6)$$

$$r'_2=r_2 - \Delta_2*\tan\alpha \quad (7)$$

It can be seen that this is a process in which radius r_2 is decreased while r_1 is increased, resulting in decreasing in the potential energy for the wheelset. However, as the process continues to go, there will come to an instance of identical rolling radius in both wheels. This is a state that the kinetic energy is at its maximum while the potential energy is zero for the wheelset lateral motion. That is to say, rolling radii of the wheelset will come to be exactly the same, i.e., $r'_1=r'_2$. Thus, we have

$$r_1 + \Delta_1*\tan\alpha=r_2 - \Delta_2*\tan\alpha \quad (8)$$

Rearranging and plugging in Δ_1 and Δ_2, the equation becomes

$$r_2 - r_1=\tan\alpha\ (2R+G)(1/\cos\Omega - 1) \quad (9)$$

Eliminating R, we get

$$1/\cos\Omega - 1=1/(G*\tan\alpha)*(r_2 - r_1)^2/(r_2 + r_1)$$

Or

$$1/\cos\Omega=1+ 1/(G*\tan\alpha)*(r_2 - r_1)^2/(r_2 + r_1) \quad (10)$$

There is a solution mathematically to Ω in the above equation. The solution can further be obtained by engineering calculations, as shown in Table 1, for some practical engineering examples. As expected, the wheel tread movement (Δ_1 and Δ_2) is about half the Δ (=0.3 inch). Note [$\Delta=(1/\tan\alpha)*(r_2- r_1)$].

Table 1. *Typical Values for Angles of the Circular Motion.*

	tan α=1/20	**Δ=0.3in**	**Gauge=56.4961 in**			
Angle=degree		**Length=inch**				
r_2=	38/2 in.	36/2 in.	34/2in.	32/2in.	30/2in.	28/2in.
r_1=	18.985	17.985	16.985	15.985	14.985	13.985
Ω=	0.117394723	0.1206129	0.1241112	0.127933	0.13213	0.13677
Δ_2=	0.149940766	0.1499375	0.1499338	0.14993	0.149925	0.14992
Δ_1=	0.150059234	0.1500625	0.1500662	0.15007	0.150075	0.15008
cosΩ=	0.999997903	0.9999978	0.9999977	0.999998	0.999997	0.999997

Table 2. *Multi-step Approximation for only r_2=19 in, r_1=18.985 in Unit: Degree, Inch.*

Step	**1**	**2**	**3**	**4**	**5**	**6**	**7**	**8**
ΔΩ	0	0.02	0.02	0.03	0.03	0.03	0.03	0.02
r'_2	19	18.9997	18.9995	18.9990	18.9984	18.9978	18.9971	18.9968
r'_1	18.985	18.9852	18.9854	18.9859	18.9865	18.9871	18.9878	18.9881
R'	71505.1	73643.4	75983.5	82034.6	89750.6	100044.	114709.	123968.

Step	**9**	**10**	**11**	**12**	**13**	**14**	**15**
ΔΩ	0.02	0.02	0.02	0.02	0.02	0.02	0.0163
r'_2	18.99645	18.99603	18.99557	18.99504	18.9944	18.99354	18.9925
r'_1	18.98855	18.98896	18.98942	18.98996	18.9906	18.99146	18.9925
R'	135815.2	151696.1	174482.6	210921.8	282144.4	514529.4	2.09E+08

The calculation proves that there exists a state in which there is no rolling radius difference for a given r_1 and r_2. Note that the calculation is carried out approximately because R and G are not updated (but they are not constant in the process). This calculation is called one-step approximation for the obvious reason. In the following, a multi-step approximation (see Table 2) will be performed in which R is updated in every step. In order to make the results converge

to the exact solution, the increment in angle Ω is taken to be very small. G is not updated in the process because conΩ ≈ 1.

Radius R' of the circular motion is calculated as

$$R'=G*r'_1/(r'_2-r'_1) \quad (11)$$

With $r'_1=r_1 + \Delta_1*\tan\alpha$, $r'_2=r_2 - \Delta_2*\tan\alpha$, $\Delta_1=R(1/\cos\Delta\Omega - 1)$ and $\Delta_2=(R+G)(1/\cos\Delta\Omega - 1)$.

where r_1, r_2 and R are taken their values from the previous step (i.e. r'_1 and r'_2).

It can be seen that, after 15 steps, rolling radius difference becomes zero ($r'_1=r'_2=18.9925$ in.) and radius of circular motion becomes ∞ (Due to numerical errors, 2.09E+8 can be viewed as ∞). That further proves that there exists a state of zero RRD.

4. Determination of the Curve of Motion for the Wheelset

We have demonstrated the motion of wheelset from the beginning (r_1- r_2 system) to a state of zero RRD. For the wheelset, this is also a state of maximum kinetic energy, see Figure 7.

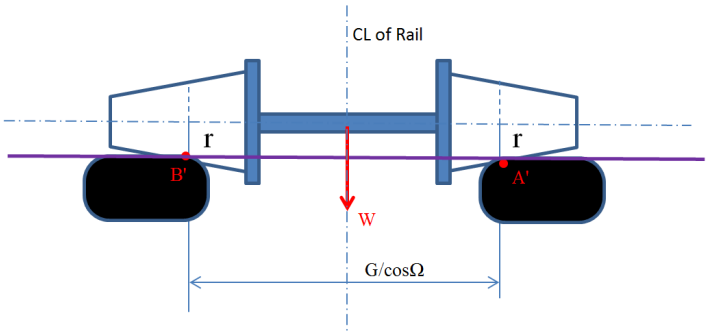

Figure 7. *State of Maximum Kinetic Energy (Zero Potential Energy).*

The change in the radius of the circular motion has been studied. However, the purpose of this study is to determine the curve of the wheelset motion. The question is that what is the curve that the wheelset has gone through so for. What we are going to do next is to compare curve of the wheelset motion to a cosine curve. If they are exactly the same, then the motion curve can be determined to sinusoidal---cosine curve. What to compare is the radii of curvature from two curves.

So far, we have made three findings about the curve of the wheelset motion.

1). Radius of curvature of the curve at the beginning (x=0) is $R=G*r_1/(r_2-r_1)$ same as Eq. 3

2). Radius of curvature of the curve at the state of zero RRD ($r'_1=r'_2$) is

$$R=\infty \quad (12)$$

3). Radius of curvature of the curve for the whole process is approximately $R'=G*r'_1/(r'_2-r'_1)$, same as Eq. 11.

For comparison, R' is calculated (Table 3) and sketched in Figure 8. For simplicity, G/2 is not added to R'.

Table 3. *One Step Approximation (Ω=0.11739 radian) for only r_2=19 in, r_1=18.985 in.*

Ω=	0	0.01467	0.02934	0.04402	0.05869	0.07337	0.08804	0.1027	0.11739
R'=	71505.184	72640.63	76274.07	83210.63	95349.62	117359.9	163476.6	305180.6	3.64E+15

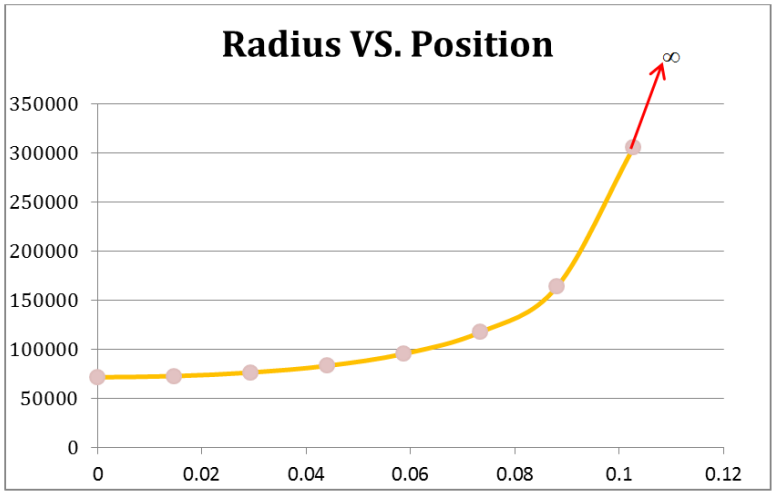

Figure 8. *Radius of Curvature R' for ¼ Cycle of Hunting.*

That is to say, the radius of curvature is R (R=71,505.1in.) at the beginning, will increase as the wheelset rolling forwards, and reaches ∞ when $r_2=r_1=r$ is reached.

The radius of curvature R is believed to match with a sinusoidal curve. Let's examine a cosine curve y.

$$y=C\cos(\omega x) \tag{13}$$

where C is the amplitude of oscillation and is half of the distance from the top to the bottom of the oscillation, ω is referred to as the circular frequency measured in radians per length and x is the horizontal distance. Note that wave length $L=(2\pi)/\omega$.

From analytical geometrics, radius of curvature for the cosine curve y can be expressed as

$$R_{cos}=|\ (1+ y'^2)^{3/2}/y''| \tag{14}$$

Plugging in y' and y'', we have

$$R_{cos}=|\ [1+(C\omega\sin\omega x)^2]^{3/2}/(C\omega^2\cos\omega x)| \tag{15}$$

By the same token, three observations can be made on the radius of curvature for the cosine curve.

1). at the beginning x=0,

$$R_{cos}=1/(C\omega^2) \tag{16}$$

The purpose is to make $R=R_{cos}$ at x=0. If we make $R=1/(C\omega^2)$, then we have $R=R_{cos}$. R is computed by Eq. (3). As will be shown later, $C=½\ (r_2 - r_1)/\tan\alpha$ (Eq. 17), and ω can be determined after R and C are computed from a given state of a r_1- r_2 system. Thus, $R=R_{cos}$ at x=0, can be satisfied.

2). at $\omega x=\pm\pi/2$, $R_{cos}=\infty$, same as Eq. 12.

3). Radius of curvature of the cosine curve for the whole process is $R_{cos}=|\ [1+(C\omega\sin\omega x)^2]^{3/2}/(C\omega^2\cos\omega x)|$, same as Eq. 15.

For comparison, R_{cos} is calculated (Table 4) and sketched in Figure 9.

Table 4. *Radius of curvature for cosine curve from 0 to π/2.*

Angle	0	0.1963	0.3926	0.5890	0.7853	0.9817	1.1780	1.3744	1.1.5707
R_{cos} in.	71506.184	72906.062	77396.68	85998.63	101123.7	128706.21	186852.5	366524.5	2.669E+12

Compared Table 3 with Table 4, we can see $R_{cos}=R'=71,506.184$ in. at the beginning, and $R_{cos}=R'=\infty$ at the end. However, values at the intermediate steps are not exactly the same but in the same pattern. They cannot be the same because values in Table 3 are approximate while those in Table 4 are exact. The only way to calculate R' can be seen so far is a step-by-step solution, and step-by-step solution is approximate.

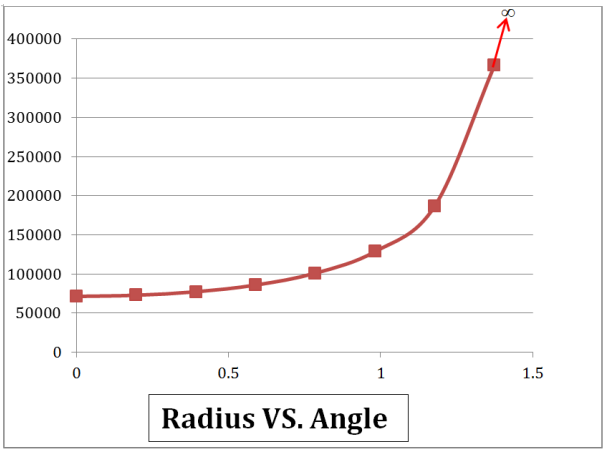

Figure 9. *Radius of Curvature R_{cos} for ¼ Cycle---0 to π/2 (1.57).*

That is to say, the radius of curvature is R_{cos} ($R_{cos}=71,505.1$in.) at the beginning, will increase as the angle becomes larger in velocity direction, and reaches ∞ when $\omega x=\pi/2$.

It has been shown that there are three common grounds between the wheelset hunting curve and a cosine curve. That is, 1) two radii of curvature are the same at the beginning, 2) two radii of curvature increase in exact the same pattern and 3) two radii of curvature reach ∞ at the end of the section. Conclusion can be drawn: wheelset hunting motion curve is the same as a cosine curve. See Figure 10.

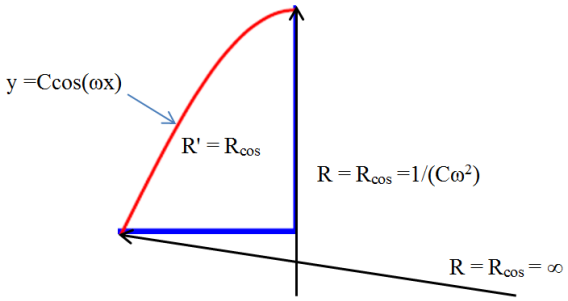

Figure 10. *Two Radii of Curvature and One-Quarter Cycle of Two Curves.*

5. Movement of Wheelset After the State of Zero RRD

The curve of wheelset motion has been proven to be sinusoidal from beginning to a state of zero RRD. What will happen to the wheelset after this state? That will be discussed in this section.

The configuration at Ω, $r'_1=r'_2$. That is, rolling radius is identical. According to the equation to calculate R, the radius of the centrifugal motion goes to ∞ due to $r'_1 - r'_2=0$. Therefore, the wheelset will go straight under this condition. That is to say, the wheelset is not in a circular motion at Ω (Note that only at Ω, the wheelset goes straight). However, the wheelset is not perpendicular to the rail; instead with angle Ω to the rail, as shown in Figure 11. This angle is very important in determining the configuration of the wheelset motion.

As stated previously the rail is straight and the wheel rail contact points on the rail are along a straight line. But this

straight line is at an angle Ω with the wheelset. Therefore, wheel rail contact points on the wheel tread must be along a straight line but at an angle Ω with the wheelset, as shown in Figure 12.

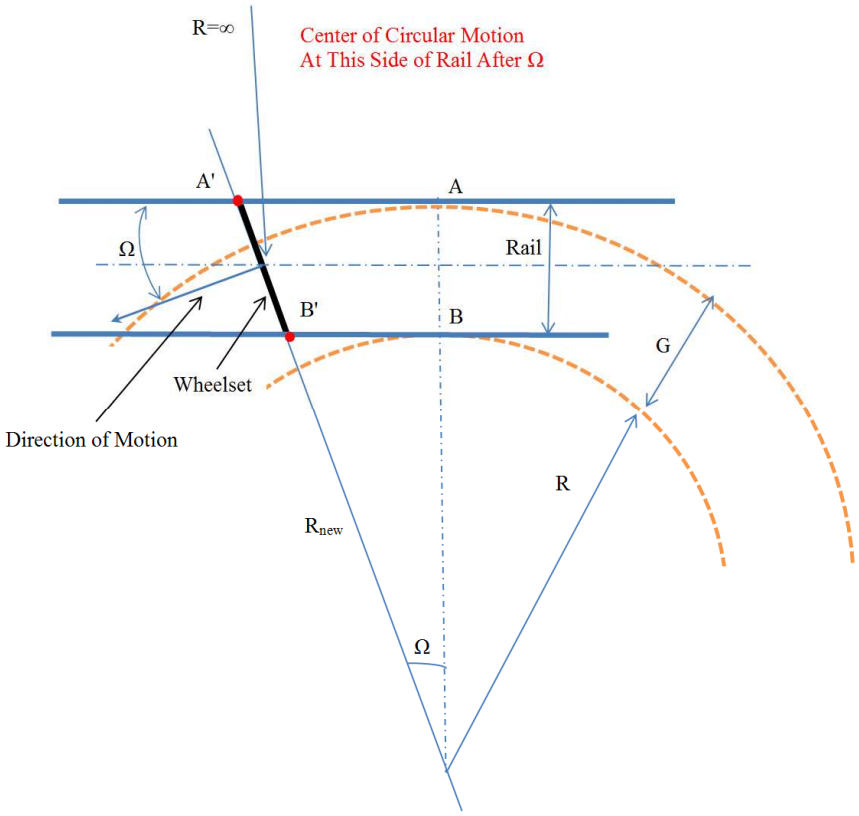

Figure 11. *Direction, Wheelset Motion at Configuration Ω [$R=G*r_1/(r_2-r_1)$, $R=\infty$ if $r_2=r_1$].*

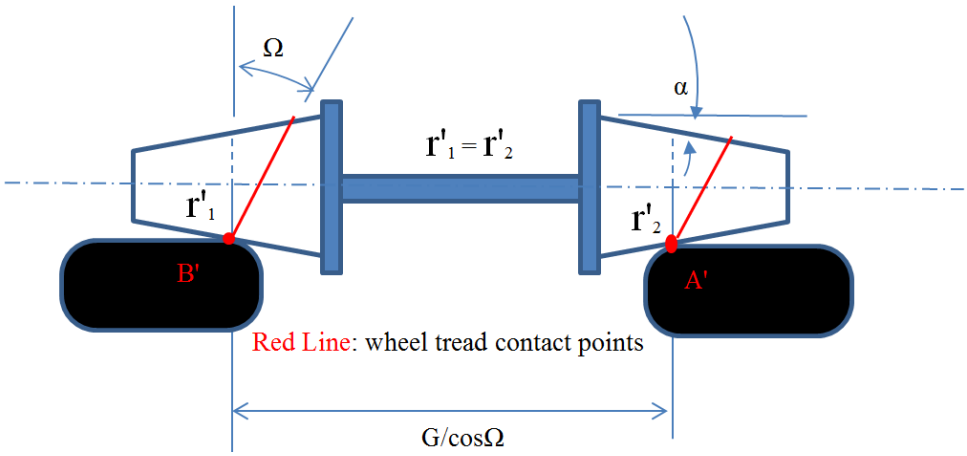

Figure 12. *Switch of Major-Minor Radii at the Configuration at Ω.*

Referring to Figure 12, one can see that rolling radius on wheel B is always larger than that on wheel A as soon as the wheelset begins to move, and that rolling radius on wheel B increases while rolling radius on wheel A decreases. (Recall that wheel A used to have the major radius while wheel B used to have the minor one in the previous process) Consequently, the wheel tread originally with r_1 now becomes the one with the major radius, and the wheel tread originally with r_2 is now the one with the minor radius. This is the switching of major-minor radii on the two wheel treads. Thus, the center (or the radius) of the centrifugal motion will switch to the other side, as shown in Figure 11. That means the curve of the wheelset circular motion will change sign, from concave to convex in this process, as shown in Figure 13.

This process will produce a new r_1 - r_2 system which is recovered from the previous r_1 - r_2 system, because of the angle Ω which is determined by the previous r_1 - r_2 system. So the curve of wheelset motion in this section is obtained by recovering the previous section, as shown in Figure 13. That is, another one-quarter of curve is added to Figure 10 to finish one half cycle of wheelset motion curve.

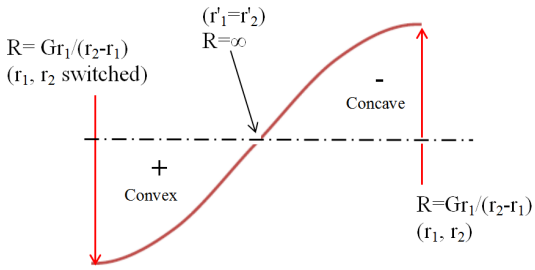

Figure 13. *Directions, Curve of Wheelset Motion of Half Cycle.*

This process will be finished when the major radius is reached r_2 and the minor radius is reached r_1, because the final stage of this process is controlled by the direction of the wheelset contact points shown in Figure 12. Furthermore, by the rule of conservation of energy, the potential energy at this stage must be same as that at the beginning state, as shown in Figure 14. Actually, conservation of energy is also the principle which will be used to determine the amplitude of the wheelset oscillation.

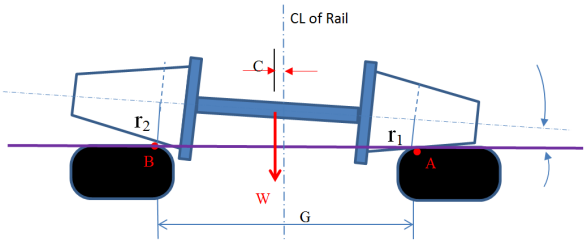

Figure 14. *State of Maximum Potential Energy (Zero Kinetic Energy Laterally).*

6. Determining the Configuration for the Curve of Wheelset Motion for One Cycle

So far, a half cycle of wheelset motion (Figure 13) has been demonstrated. The other half part of the motion is an exact repeat of this first half. The only diffference is that radius of curve R is in opposite direction to begin with. Thus, the pattern of the motion will be the same but in the opposite direction. That is to say, for the new r_1 - r_2 system, as the circular motion continues to go, rolling radius r_2 will decrease while r_1 will increase. Thus, R will increase and become infinite (∞) when r_2=r_1. Then the major and minor radii will switch to the other wheel tread as the motion going on. Finally, another r_2 - r_1 system will be established, which is exactly the same as the one in the beginning of the hunting. Therefore, one cycle of hunting oscillation can be produced by mirroring the half cycle motion curve in Figure 13, as shown in Figure 15.

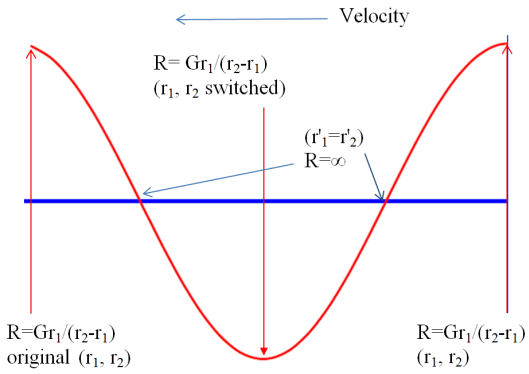

Figure 15. *Cosine Curve for One Cycle of Wheelset Hunting.*

Thus we have produced the whole curve for wheelset hunting motion because the rest of hunting is just a repeat of this cycle. Wheelset configurations in one cycle of hunting oscillation is sketched in Figure 16. After the derivation of the hunting curve, one important observation can be made. All the wheelset configurations in Figure 16 will start a hunting motion, and the hunting curve can be described by the same cosine curve. That is to say, wheelset configurations can be at1, 2 and 3, or anywhere between the hunting cycle, wheelset hunting will be initiated. So there are many wheelset configurations can start a hunting motion not just one as described in Klingel's formula.

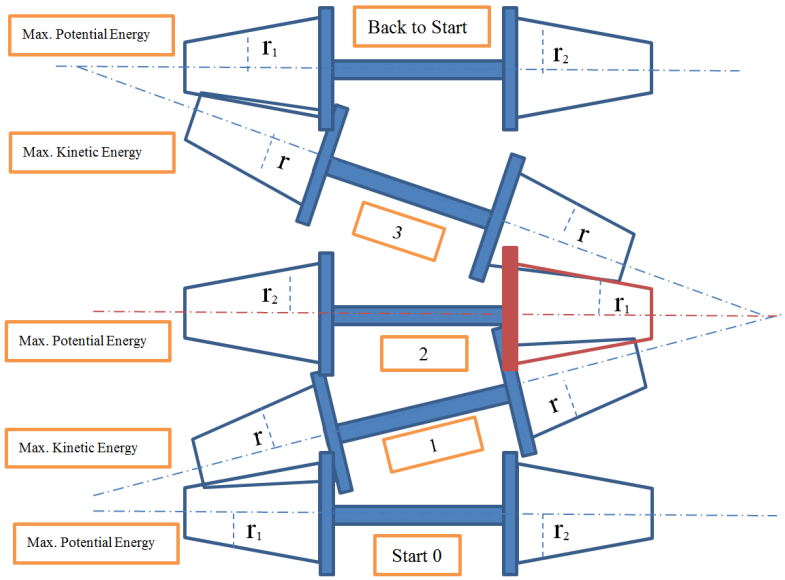

Figure 16. *Wheelset Hunting Motion in One Cycle.*

7. Wave Length and Vibration Frequency of Hunting for the Wheelset

We have determined that wheelset hunting motion is sinusoidal [y=Ccos(ωx)] and constructed one cycle of the curve. However, C and ω (amplitude and frequency of the oscillation) of the curve have not been determined yet. C is the lateral displacement of the wheelset and can be determined as follows:

$$C=½ (r_2 - r_1)/\tan\alpha \quad (17)$$

1). At x=0, as shown previously, the radius of curvature for $y=C\cos(\omega x)=C\cos(2\pi x/L)$ is $R_{cos}=1/(C\omega^2)$, same as Eq. 16.

2). At the beginning of hunting, the radius of curvature determined by r_1 and r_2 is again $R=G*r_1/(r_2-r_1)$, same as Eq. 3.

Make $R_{cos}=R+G/2$. Therefore, $\omega^2=1/(C*R_{cos})$. Plugging in C and R_{cos}, we have

$$\omega^2=4*\tan\alpha/[G(r_2+r_1)] \quad (18)$$

With $\omega=2\pi/L$, the exact wave length (L) can be obtained theoretically,

$$L=\pi*\{[G(r_1 + r_2)]/\tan\alpha\}^{1/2} \quad (19)$$

Note that Eq. 19 is the same as Eq. 1. For the purpose of proving the theoretical values and comparison, the wave length will be calculated by numerical operations. From Figures 4 & 5, as the major radius decreases while the minor radius increases there will come to a point that two radii are the same, such that ¼ of wave length has passed. It can be seen that the ¼ of wave length is finished after a certain number of wheelset rotations. So the wave length depends only on the number of wheel rotations and the number depends on r_1 and r_2. Therefore, the wave length is independent on the train velocity. That means the truck will have the same wave length of hunting even though the truck moving with different velocities. The faster the truck goes, the quicker the truck will go over the distance of the wave length.

It is important to realize that the center line of hunting is coincident with the center line of the gauge. With referring to Figure 5, we can see that the length of line $C_cC'_c$ represents ¼ of the wave length of wheelset hunting. Therefore, we can calculate the wave length approximately,

$$L_a=4*(R+G/2)*\tan\Omega$$

$$=2G*\tan\Omega*(r_2 + r_1)/(r_2 - r_1) \quad (20)$$

Table 5. *Typical Values for L_a and L of the Hunting Motion.*

	tan α=1/20	Δ=0.3in	Gauge=56.4961 in			
Angle=degree		**Length=inch**				
r_2=	38/2 in.	36/2 in.	34/2in.	32/2in.	30/2in.	28/2in.
r_1=	18.985	17.985	16.985	15.985	14.985	13.985
Ω=	0.117394723	0.1206129	0.1241112	0.127933	0.13213	0.13677
L_a	828.8508154	806.7442	784.01449	760.6058	736.4535	711.4818
L	650.8486	633.48263	615.62691	597.2376	578.2638	558.6459

It can be seen from the calculation (Table 5.) that the wave lengths L_a (approximate) and L (theory) of hunting oscillation are decreased as the radius of the wheel is decreased. It is reasonable that the estimated wave length L_a is larger than the exact theoretical one, because the radius R and the orientation of the wheelset do not change in the estimation. A step-by-step solution will produce an estimated L_a closer to the theoretical wave length L, but L_a is always an approximate.

8. Conclusions and Construction of a Total Solution to Hunting

Wheelset hunting can begin with a circular motion. However, the radius of the centrifugal motion will be altered continuously during the motion, from R to ∞ in magnitude and from lateral to longitudinal in direction. During this process, the major rolling radius continuously decreases while the minor rolling radius increases until the major and minor are equal ($r_2=r_1$). Then the major and minor rolling radii will switch to the other wheel tread as the motion continues. Thus, the same centrifugal motion will be reversed to the other side of the rail. That the switching can occur is because both the changing of radius R and a mechanism at $r_2=r_1$. The mechanism also guarantees the reversed centrifugal motion is exactly the same as the previous one but in the opposite direction.

The radii of curvature at two end points of the hunting (one cycle) curve are calculated exactly and found to be the same as those of a cosine curve. Meanwhile, for the points in between (the end points), the radii of curvature of the hunting curve are expected to have a small difference with those of a cosine curve due to the exact values not being the same as the estimated (calculated) values. Note that the curve patterns (Figures 7&8) are the same. So the radii of curvature for the two curves are the same. The motion of the wheelset in hunting is therefore a cosine curve. One cycle of hunting curve is constructed and parameters for the sinusoidal curve are determined in the paper. From the derivation of the hunting curve, Figure 16, one observation can be made---Any wheelset configurations on the rail can start a hunting motion not just one as described in Klingel's formula. Thus, hunting of the wheelset begins as soon as the wheelset begins to move.

More interestingly, without wheelset conicity, it has found that the high speed trains will hunt in service operations also. Theoretically, there always exists the rolling radius difference even if the wheel coinicity does not exist. That is why truck lateral motion will always occur no matter how good the equipment is because unevenness always exists.

This research lays the foundation for the continuous research on truck/wheelset hunting in the future. Thus, a total solution to the hunting problems can be created, which is impossible with Klingel's theory. The following major hunting problems have been solved.

1) Even though millions of trucks have been manufactured, theoretical calculation of dynamic loading for truck design has never been established. There is no theoretical base found for people to do the calculation. However, the train/truck critical speed in hunting was calculated by many researchers [16], but only one critical speed for one load case. Actually, there are three critical speeds in one load case. Both dynamic loading and critical speeds in three directions for a truck can be calculated to use in truck design [10].
2) Wheelset hunting motion curve while curving can be analyzed and generated [8], which is impossible before. That is, Klingel's theory cannot do anything about that.
3) There are usually two or more wheelsets in a truck. Wheelsets in a truck will fight against each other to reduce hunting. That is why a single-wheelset-truck will have a severe hunting problem. We can now analyze and evaluate the interaction between wheelsets in a truck [9].
4) A common question asked in the railroad is "Why trains stay on tracks?" [15]. Wheelset balance velocity [1] can explain why. Testing finds that a tapered wheelset will derail at its balance velocity [13].
5) Wheelset balance velocity can be used to analyze the root cause of rail corrugations, and to do inspections for a worn wheelset scientifically and mathematically. Wheelset hunting can be eliminated by a hunting eliminator [13].
6) Coefficients of friction---static versus dynamic [14], Sliding friction and rolling friction [11], Derailment modes [4, 5] and Braking distance calculation (a thousand year old problem) [12], all these have been solved, with more to come.

References

[1] J. Y. Huang, "Dynamic Analysis for Railroad Truck Design", Draft Paper, 2008 IEEE/ASME Joint Rail Conference, April 22-23, 2008 Wilmington, Delaware, USA.

[2] A. H. Wickens, "Fundamentals of Railway Vehicle Dynamics: Guidance and Stability", Taylor & Francis e-Library, 2005.

[3] A. H. Wickens, Chapter 2 "A History of Railway Vehicle Dynamics", Handbook of Railway Vehicle Dynamics, Edited by Simon Iwnicki, Taylor & Francis Group LLC, 2006.

[4] J. Y. Huang, "Nadal's Limit (L/V ratio) to Wheel Climb and Two derailment Modes", Engineering Physics. Vol. 5, No. 1, 2021, pp. 8-14. doi: 10.11648/j.ep.20210501. ISSN: 2640-1010 (Print); ISSN: 2640-1029 (Online). 12May 2021.

[5] J. Y. Huang, "The Boundary of Nadal's Limit (L/V ratio) and Commencing Wheel Derailment for Railroad Truck", Draft Paper, 2008 IEEE/ASME Joint Rail Conference, April 22-23, 2008 Wilmington, Delaware, USA.

[6] Bosso et al, "Mechatronic Modeling of Real-Time Wheel–Rail Contact", 2013, ISBN 978-3-642-36245-3, http://www.springer.com/978-3-642-36245-3.

[7] J. Y. Huang, "Constraint on Angle of Attack During Curving of Railroad Truck", Draft Paper, 2008 IEEE/ASME Joint Rail Conference, April 22-23, 2008 Wilmington, Delaware, USA.

[8] J. Y. Huang, "Analysis of Wheelset Hunting in Curving", Company Research paper, High Tech Pressure Safety, USA, 2015.

[9] J. Y. Huang, "Truck Wheelset Interaction in Hunting", Company Research paper, High Tech Pressure Safety, USA, 2015.

[10] J. Y. Huang, "Hunting Excitation and Response of a Truck---Truck Dynamic Loading and Critical Speeds", Company Research paper, High Tech Pressure Safety, USA, 2016.

[11] J. Y. Huang, "Sliding Friction and Rolling Friction of a Wheel", Company Research paper, High Tech Pressure Safety, USA, 2017.

[12] J. Y. Huang, "Braking Behaviors and Calculations for Railroad Wheel", Company Research paper, High Tech Pressure Safety, USA, 2017.

[13] J. Y. Huang, "Balance Velocity of Tapered Wheelset and Hunting Eliminator", Presentation, 2021 IEEE/ASME Joint Rail Conference, USA.

[14] J. Y. Huang, "Coefficients of Friction --- Static versus Dynamic", 2020 IEEE/ASME Joint Rail Conference, St. Louis, Missouri, USA.

[15] B. Shayak, "Why trains stay on tracks", American Journal of Physics 85, 178 (2017); https://doi.org/10.1119/1.4973370.

[16] J. Gerlici1 eta, "Calculated estimation of railway wheels equivalent conicity influence on critical speed of railway passenger car", MATEC Web of Conferences 157, 03006 (2018), https://doi.org/10.1051/matecconf/201815703006.